AD_____

Award Number: W81XWH-04-1-0344

TITLE: Targeting of the Nuclear Receptor Coactivator Isoform Delta3AIR in Breast Cancer

PRINCIPAL INVESTIGATOR: Aparna Mani

CONTRACTING ORGANIZATION: Georgetown University Medical Center
Washington, DC 20007

REPORT DATE: March 2005

TYPE OF REPORT: Annual Summary

PREPARED FOR: U.S. Army Medical Research and Materiel Command
Fort Detrick, Maryland 21702-5012

DISTRIBUTION STATEMENT: Approved for Public Release;
Distribution Unlimited

The views, opinions and/or findings contained in this report are those of the author(s) and should not be construed as an official Department of the Army position, policy or decision unless so designated by other documentation.

REPORT DOCUMENTATION PAGE

Form Approved
OMB No. 074-0188

1. AGENCY USE ONLY (Leave blank)	2. REPORT DATE	3. REPORT TYPE AND DATES COVERED
	March 2005	Annual Summary (23 Feb 2004 - 22 Feb 2005)

4. TITLE AND SUBTITLE
Targeting of the Nuclear Receptor Coactivator Isoform Delta3AIR in Breast Cancer

5. FUNDING NUMBERS
W81XWH-04-1-0344

6. AUTHOR(S)
Aparna Mani

7. PERFORMING ORGANIZATION NAME(S) AND ADDRESS(ES)
Georgetown University Medical Center
Washington, DC 20007

E-Mail: Am2@georgetown.edu

8. PERFORMING ORGANIZATION REPORT NUMBER

9. SPONSORING / MONITORING AGENCY NAME(S) AND ADDRESS(ES)
U.S. Army Medical Research and Materiel Command
Fort Detrick, Maryland 21702-5012

10. SPONSORING / MONITORING AGENCY REPORT NUMBER

11. SUPPLEMENTARY NOTES

12a. DISTRIBUTION / AVAILABILITY STATEMENT
Approved for Public Release; Distribution Unlimited

12b. DISTRIBUTION CODE

13. ABSTRACT (Maximum 200 Words)

AIB1 which stands for "Amplified in Breast cancer", codes for a protein that is a member of the steroid receptor coactivator (SRC) family. AIB1 is amplified in approximately 5-10% of breast cancers and the mRNA and protein overexpressed in >30% of breast cancers. AIB1 interacts with a superfamily of ligand activated nuclear receptors to potentiate transcriptional activity leading to upregulation of downstream target gene expression. An important finding was that an isoform of AIB1 (Δ3AIB1) is a significantly more effective coactivator of the estrogen receptor than AIB1 and is highly overexpressed in human breast cancer. Prior work in our lab showed that the downregulation of overall levels of AIB1 plus Δ3AIB1, using a regulatable AIB1 directed ribozyme, resulted in reduced tumor growth *in vivo*. Overall, these data indicate a major role for AIB1 and its isoform Δ3AIB1 in breast cancer development and growth. However the relative roles of AIB1 versus the more highly active Δ3AIB1 in phenotypic changes in the breast has not been determined. In this investigation, we are developing a method to use siRNA directed at Δ3AIB1 in order investigate its role in breast cancer and as a possible future therapeutic approach to breast cancer.

14. SUBJECT TERMS
No subject terms provided.

15. NUMBER OF PAGES
21

16. PRICE CODE

17. SECURITY CLASSIFICATION OF REPORT	18. SECURITY CLASSIFICATION OF THIS PAGE	19. SECURITY CLASSIFICATION OF ABSTRACT	20. LIMITATION OF ABSTRACT
Unclassified	Unclassified	Unclassified	Unlimited

Table of Contents

INTRODUCTION

Of particular interest to breast cancer was the discovery that an area of chromosome 20q, known to be frequently amplified in breast cancer, harbored the gene for AIB1. AIB1 which stands for " **A**mplified **i**n **B**reast cancer" codes for a protein which is a member of the steroid receptor coactivator (SRC) family. AIB1 is amplified in approximately 5-10% of breast cancers and the mRNA and protein overexpressed in >30% of breast cancers. AIB1 interacts with a superfamily of ligand activated nuclear receptors including the estrogen receptor (ER) and progesterone receptor (PR) to potentiate transcriptional activity leading to upregulation of downstream target gene expression. An important finding was that an isoform of AIB1 (Δ3AIB1) is a significantly more effective coactivator of the estrogen receptor than AIB1 and is highly overexpressed in human breast cancer. Prior work in our lab showed that the downregulation of overall levels of AIB1 plus Δ3AIB1, using a regulatable AIB1 directed ribozyme, resulted in reduced tumor growth *in vivo*. Overall, these data indicate a major role for AIB1 and its isoform Δ3AIB1 in breast cancer development and growth. However the relative roles of AIB1 versus the more highly active Δ3AIB1 in phenotypic changes in the breast has not been determined. Specifically, the research done with the funding of this grant will examine and compare the effects of selective reduction in the gene expression of isoform Δ3AIB1 by siRNA versus the phenotypic responses to siRNA directed at both AIB1/Δ3AIB1. Ultimately, the information from this study will be used as a basis for the development of AIB1 and Δ3AIB1 directed siRNA as a potential therapy in humans.

BODY

Task 1: Design small interfering siRNA molecules that specifically target the nuclear receptor coactivator isoform Δ3AIB1.

As a prelude to designing and developing siRNA molecules that specifically target the Δ3AIB1 isoform, we developed primers to specifically detect the Δ3AIB1 isoform by the technique of real-time PCR. The primer sequence specific for Δ3AIB1 overlaps the exon 3 splice junction. We tried different primers across the splice junction at different temperatures and different concentrations. Surprisingly the primer that was overlapping just one base pair across the splice junction (labeled SJ1) gave the best results. (Figure 1) We used beta-actin and GAPDH to normalize for RNA loading. Our results showed that for both the Δ3AIB1 plasmid control and several breast cancer cell lines, including MCF-7 and MCF10A, we were able to pick up a signal for Δ3AIB1.

CGGCGGCGGCTGCGGCTTAGTCGGTGGCGGCCGGCGGCGGCTGCGGGCTGAGCGGCGAGTTTCCG

ATTTAAAGCTGAGCTGCGAGGAAAATGGCGGCGGGAGGATCAAAATACTTGCTGGATGGTGGACT **Exon 1**

CAGAGACCAATAAAAATAAACTGCTTGAACATCCTTTGACTGGTTAGCCAGTTGCTGATGTATAT

TCAAGATGAGTGGATTAGGAGAAAACTTGGATCCACTGGCCAGTGATTCACGAAAACGCAAATTG **Exon 2**

SJ1 →

CCAT**GTGATACTCCAGGACAAGG**TCTTACCTGCAGTGGTGAAAAACGGAGACGGGAGCAGGAAAG **Exon 3**

TAAATATATTGAAGAATTGGCTGAGCTGATATCTGCCAATCTTAGTGATATTGACAATTTCAATG

TCAAACCAGATAAATGTGCGATTTTAAAGGAAACAGTAAGACAGATACGTCAAATAAAAGAGCAA

SJ1 1 bp overhang with exon 4

G**G**AAAAACTATTTCCAATGATGATGATGTTCAAAAAGCCGATGTATCTTCTACAGGGCAGGGAGT **Exon 4**

← 541R

TATTGATAAAGACTCCTT**AGGACCGCTTTTACTTCAGG**CATTGGATGGTTTCCTATTTGTGGTGA

ATCGAGACGGAAACATTGTATTTGTATCAGAAAATGTCACACAATACCTGCAATATAAGCAAGAG

GACCTGGTTAACACAAGTGTTTACAATATCTTACATGAAGAAGACAGAAA

Figure 1: The N-terminal cDNA nucleotide sequence of AIB1 obtained from PubMed (accession number AF0102108) with both the forward primer (SJI) and reverse primer (541R) indicated in bold. The forward primer SJ1 overlaps just 1 base pair across the splice junction between exon 2 and exon 4.

Task 2: To determine if siRNA reduction of cellular levels of AIB1 of Δ3AIB1 can change the phenotype of breast cancer cell lines. (Please see appended reprint.)

I have worked with Dr. Annabell Oh on a study in which siRNA directed at nucleotides 564-582 of AIB1 to selectively reduce AIB1 gene expression in the MCF-7 breast cancer cell line. This study resulted in a recent publication in the journal *Cancer Research.* In this study we found that when AIB1 levels were knocked down with siRNA, this resulted in a significant decrease in IGF-1 induced anchorage independent growth of MCF-7 breast cancer cells in soft agar. (Figure 2A – taken from appended reprint Oh et al, *Cancer Research* v64:8299, 2004.)[1]

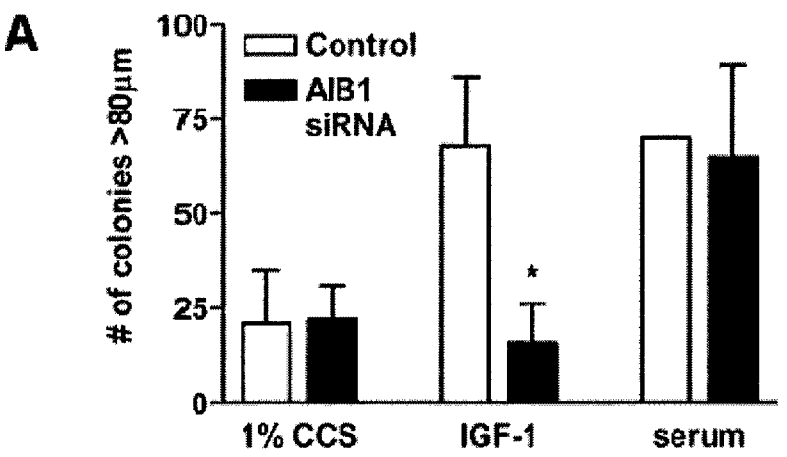

Figure 2: AIB1 is critical for anchorage independent growth and colony formation of MCF-7 breast cancer cells. A pool of MCF-7 cells was transfected with either siRNA directed against AIB1 or a control siRNA for 24 hours. The transfected cells were then plated in soft agar dishes in the absence (1% CCS) or presence of IGF-1 or fetal bovine serum (serum). The colonies were measured after ~2 weeks.

We are currently in the process of developing siRNA directed specifically against the Δ3AIB1 isoform and we plan to complete similar using this siRNA.

Task 3: To determine if Δ3AIB1 siRNA is effective *in vivo*.

We have not formally begun this task since we are awaiting the development of the Δ3AIB1 siRNA. Currently other members in our lab have developed an *in vivo* assay in the chicken embryo in which they are using siRNA to target and posttranscriptionally knockdown other genes. For this assay chicken embryos are grown outside their shells in Petri dishes and transfections are carried out according to the protocol of Tuschl.[2] We plan to carry out similar studies in which we use siRNA directed against AIB1 versus siRNA specifically directed against Δ3AIB1 in the chicken embryo.

KEY RESEARCH ACCOMPLISHMENTS

Development of real time PCR assay to specifically detect Δ3AIB1 isoform versus AIB

REPORTABLE OUTCOMES

"The Nuclear receptor coacvtivator AIB1 mediates Insulin-like Growth Factor 1-Induced Phenotypic Changes in Human Breast Cancer Cells." Annabell Oh, Heinz Joachim List, Ronald Reiter, **Aparna Mani**, Ying Zhang, Edmund Gehan, Anton Wellstein, and Anna T. Riegel, *Cancer Research.* 2004 Nov 15, 64:8299-8308.

CONCLUSIONS

The work done to date as outlined in this report illustrates that it is possible to specifically detect the Δ3AIB1 isoform versus AIB1 by real time PCR. This gives us an initial idea of how to design and develop siRNA to specifically target Δ3AIB1. In addition, we plan to continue studies on the effects of AIB1 on growth of breast cancer cells using the siRNA we have already developed for AIB1.

REFERENCES

1. Oh S, et al., *Cancer Research* **64**, 8299-8308 (2004)

2. Tuschl T. (2002) http://www.mpibpc.gwdg.de/abteilungen/100/105/sirna.html

[CANCER RESEARCH 64, 8299–8308, November 15, 2004]

The Nuclear Receptor Coactivator AIB1 Mediates Insulin-like Growth Factor I-induced Phenotypic Changes in Human Breast Cancer Cells

Annabell Oh,[1] Heinz-Joachim List,[1] Ronald Reiter,[1] Aparna Mani,[1] Ying Zhang,[2] Edmund Gehan,[2] Anton Wellstein,[1] and Anna T. Riegel[1]

Departments of [1]Oncology and [2]Biostatistics, Vincent T. Lombardi Cancer Center, Georgetown University, Washington, District of Columbia

ABSTRACT

The nuclear receptor coactivator AIB1 (amplified in breast cancer 1) is overexpressed in human breast cancers and is required for estrogen signaling. However, the role of AIB1 in breast cancer etiology is not known. Here, we show that AIB1 is rate-limiting for insulin-like growth factor I (IGF-I)-dependent phenotypic changes and gene expression in human breast cancer cells. Reduction of endogenous AIB1 levels by small interfering RNA in MCF-7 breast cancer cells prevented IGF-I–stimulated anchorage-independent growth by reducing IGF-I–dependent anti-anoikis. cDNA array and immunoblot analysis of gene expression revealed that reduction in AIB1 levels led to a significant decrease in the expression of several genes controlling the cell cycle and apoptosis. These AIB1-dependent changes were also observed in the presence of estrogen antagonist and were corroborated in the estrogen receptor-negative cell line MDA MB-231. AIB1 reduction decreased the expression of the IGF-I receptor and IRS-1 in MCF-7 but not in MDA MB-231 cells. IGF-I–stimulated activation of AKT was reduced by AIB1 small interfering RNA treatment, whereas mitogen-activated protein kinase (extracellular signal-regulated kinase 1/2) activation by IGF-I was unaffected. We conclude that AIB1 is required for IGF-I–induced proliferation, signaling, cell survival, and gene expression in human breast cancer cells, independent of its role in estrogen receptor signaling.

INTRODUCTION

The nuclear receptor coactivator AIB1 belongs to the p160/SRC (steroid receptor coactivator) family consisting of SRC-1 (1), TIF-2 (GRIP1; ref. 2) and AIB1 (ref. 3; ACTR/RAC3/TRAM-1/SRC-3; refs. 4–7). The AIB1 gene is amplified in several human cancers, such as breast, ovarian, pancreatic, and gastric cancer (3, 8, 9). Amplification of the AIB1 gene is detected in 5 to 10% of primary breast tumors and AIB1 is highly expressed in many breast tumor specimens (3, 10–12). AIB1 enhances *in vitro* the transcriptional activity of the estrogen receptor (ER; refs. 3, 4, 7) and binds directly to ER *in vivo* (13). Furthermore, AIB1 is rate-limiting for estrogen-mediated growth of MCF-7 human breast cancer cells (14). AIB1 gene expression is up-regulated by selective ER modulators, such as tamoxifen (15) and the estrogenic activity of selective ER modulators, can be increased by AIB1 and an AIB1 isoform (16). However, emerging data suggest that the role of AIB1 is not restricted to nuclear receptor signaling. Disruption of p/CIP, the mouse homologue of AIB1, results in a pleiotropic phenotype, including reduced female reproductive function and blunted mammary gland development in mice (17, 18). Interestingly, embryonic tissues from p/CIP-knockout mice show severe defects in the insulin-like growth factor I (IGF-I) and growth hormone-signaling pathways (18). Consistent with this role for AIB1 in growth factor signaling, we have found that an isoform of AIB1 (Δ3-AIB1) overexpressed in breast tumors strongly enhances epidermal growth factor-mediated transcription in squamous cell carcinoma cells (19). Also, AIB1 overexpression is positively correlated with the expression of p53 and HER2/neu in breast tumors (20). p/CIP also plays a role in CREB binding protein–dependent transcriptional activation induced by IFN-γ and 12-*O*-tetradecanoylphorbol-13-acetate (21), and a study of Taiman, the Drosophila homologue of AIB1, indicates that AIB1 is also involved in the control of cell motility as well as platelet-derived growth factor/vascular endothelial growth factor signaling (22, 23). Taken together, these data suggest that AIB1 may well be an important factor for growth factor-mediated signaling pathways. In this study, we report that selective reduction of endogenous AIB1 levels in MCF-7 cells reveals a significant role for this coactivator in IGF-I signaling in human breast cancer cells.

MATERIALS AND METHODS

Cell Culture and Reagents. MCF-7 and MDA MB-231 human breast cancer cells were maintained in Improved Modified Eagle's Medium (IMEM; Invitrogen, Carlsbad, CA) with 10% fetal bovine serum. Recombinant human IGF-I (R&D Systems, Minneapolis, MN) was resuspended in 10 mmol/L acetic acid +0.1% bovine serum albumin and used at 100 ng/mL (13 nmol/L). ICI 182,720 (Tocris Cookson, Ellisville, MO) was resuspended in etomidate and used at a concentration of 10 nmol/L.

Small Interfering (si)RNA Design. Twenty-one–mer oligoribonucleotides of sense and antisense RNA strands were synthesized corresponding to nucleotides 564–582 of the AIB1 coding region. The AIB1 sense oligoribonucleotide sequence as follows: r(GGUGAAUCGAGACGGAAAC)dTT. The AIB1 antisense oligoribonucleotide sequence as follows: r(GUUUCCGUCUCGAUUCACC)dTT. The control siRNA is a scrambled sequence and does not target any known mammalian mRNA (Qiagen, Valencia, CA). The control sense oligoribonucleotide sequence as follows: r(UCCGUUUCGGUCCACAUUC)dTT. The control antisense oligoribonucleotide sequence as follows: r(GAAUGUGGACCGAAACGGA)dTT (Qiagen). The lyophilized double-stranded RNA was reconstituted in 1 mL of annealing buffer [100 mmol/L potassium acetate, 30 mmol/L HEPES-KOH, 2 mmol/L magnesium acetate (pH 7.4)], giving a final concentration of 20 μmol/L. The solution was then heated for 1 minute at 90°C and incubated at 37°C for 60 minutes.

Attached Cell Proliferation, Cell Cycle, and Apoptosis Assays. For siRNA experiments, 24 hours before transfection, MCF-7 cells were plated in a 10-cm dish at 50% confluency in IMEM +10% FBS. For each transfection, 60 μL of 20 μmol/L AIB1 siRNA were diluted with 1 mL of IMEM plus 60 μL of Oligofectamine (Invitrogen). The siRNA and Oligofectamine solutions were allowed to complex at room temperature for 15 minutes before treatment of the cells. After washing, the siRNA-Oligofectamine complex was added to the cells in 5 mL of IMEM and incubated for 4 hours at 37°C. A total of 1.5 mL of IMEM +30% FBS was added to the transfected cells and incubated for 16 to 18 hours at 37°C. For proliferation assays, the transfected cells were trypsinized and placed into 96-well plates and treated with IMEM +1% charcoal-stripped calf serum (CCS) containing 100 ng/mL IGF-I or 10% FBS (serum). Cell number was determined by a WST-1 colorimetric assay (Roche Diagnostics, Indianapolis, MN). For cell cycle or apoptosis analysis, the transfected cells were trypsinized and placed into 60-mm dishes and treated with IMEM +1% CCS with 100 ng/mL IGF-I or 10% FBS for 24 hours. Cell cycle analysis was done with the Vindelov method of nuclei preparation for flow cytometry DNA analysis. The percentage of cells in early and late

Received 2/3/04; revised 9/11/04; accepted 9/20/04.

Grant support: Breast Cancer Research Program of the Department of Defense Awards DAMD17-99-1-9203 (A. Riegel), DAMD17-02-1-0394 (A. Oh), and DAMD17-99-1-9204 (H-J. List).

The costs of publication of this article were defrayed in part by the payment of page charges. This article must therefore be hereby marked *advertisement* in accordance with 18 U.S.C. Section 1734 solely to indicate this fact.

Requests for reprints: Anna T. Riegel, Department of Oncology, Vincent T. Lombardi Cancer Center Research Building, E307, Georgetown University, 3970 Reservoir Road, Washington, D.C. 20057, Phone: (202) 687-1479; Fax: (202) 687-4821; E-mail: ariege01@georgetown.edu.

apoptosis (percent cell death) was analyzed by staining with Annexin V-FITC (Trevigen, Inc., Gaithersburg, MD).

Soft Agar Colony Formation Assay. MCF-7 cells were transfected with either AIB1 or control siRNA as described from the siRNA proliferation assays. After 16 to 18 hours, 7000 cells were resuspended in 0.35% soft agar and layered on top of 1 mL of 0.6% solidified agar in a 35-mm dish with 100 ng/mL IGF-I or 10% FBS (serum). IMEM +1% CCS were included in both layers. The soft agar colonies were allowed to grow at 37°C for 10 to 15 days. Cell colonies with a diameter of ≥ 80 μm were counted with an image analyzer (Omnicon TCA, Biologics, Gainesville, VA). Experiments were carried out in triplicate.

Cell Suspension Cell Cycle and Apoptosis Assays. To prevent cell attachment, 60-mm dishes were coated with 10 mg/mL poly(2-hydroxyethyl methacrylate; poly-HEMA, Sigma-Aldrich, St. Louis, MO) diluted in etomidate and allowed to dry completely. Estrogen-stripped MCF-7 cells were transfected with AIB1 or control siRNA as described above for the proliferation assays. After 48 hours, the transfected cells were plated onto the poly-HEMA coated dishes in IMEM +1% CCS with 100 ng/mL IGF-I or 10% FBS (serum). After 24 hours, the cells were harvested either for cell cycle analysis or apoptosis analysis as described above. Each experiment was carried out in duplicate.

Western Blot Analysis. Attached cells were transfected with siRNA and treated with growth factors for 48 hours. Unattached cells (poly-HEMA), a pool of MCF-7 or MDA MB-231 cells, was transfected with siRNA under normal adherent culture conditions. After 24 hours, the transfected cells were trypsinized, washed in 5% CCS + IMEM, and plated in poly-HEMA coated dishes for 24 hours with appropriate treatment media. Cells were then washed with cold PBS, lysed in 50 mmol/L Tris-HCl (pH 8.0), 150 mmol/L NaCl, 40 mmol/L β-glycerophosphate-Na, 0.25% Na-deoxycholate, 1% NP40, 50 mmol/L NaF, 20 mmol/L Na PP_I, 1 mmol/L EGTA, 1 mmol/L Na_3VO_4, and 1× complete protease inhibitor (Roche Diagnostics) and incubated on ice for 20 minutes. The lysate was centrifuged at 10,000 × g at 4°C for 15 minutes. The lysate was boiled in SDS-PAGE buffer with reducing agents, proteins were resolved by electrophoresis on a 4 to 20% Tris-glycine gel, transferred to a polyvinylidene difluoride membrane, and the membrane was incubated for 1 hour at room temperature with 5% milk in PBST (PBS, 0.2% Tween 20). Primary and secondary antibodies were diluted in 5% milk in PBST, and incubations were done at room temperature for 1 hour. The antibodies used were raised against: AIB1 (BD Transduction Laboratories, San Jose, CA); β-actin (Chemicon International, Inc., Temecula, CA); IRS-1 (Upstate, Lake Placid, NY); IRS-2 (Upstate); ER-α clone 1D5 (DakoCytomation, Carpinteria, CA); cyclin D1 (Neomarkers/Lab Vision, Fremont, CA); Bcl-2 (Santa Cruz Biotechnology, Santa Cruz, CA); and IGF-I receptor (IGF-IR) α, HER2/erbB2, phospho-AKT (Ser^{473}), AKT, phospho-p44/42 MAPK (Thr^{202}/Tyr^{204}), and p44/42 MAPK (Cell Signaling Technologies, Beverly, MA). Relative band intensities were assessed with densitometry and corrected for β-actin loading.

Real-Time Reverse Transcription-PCR. Total RNA was extracted and DNase treated with the RNeasy Mini kit (Qiagen). Real-time reverse transcription-PCR was done with the SuperScript One-Step Reverse Transcription-PCR with Platinum Taq system (Invitrogen). Samples were reverse transcribed for 30 minutes at 58°C, followed by a denaturing step at 95°C for 5 minutes and 40 cycles of 15 s at 95°C and 1 minute at 58°C. Fluorescence data were collected during the 58°C step with the Cycler iQ Detection System (Bio-Rad Laboratories, Hercules, CA). The primers and probes for real-time reverse transcription-PCR measurement were as follows: AIB1 forward primer, 5′-CAGTGATTCACGAAAACGCA-3′; AIB1 reverse primer, 5′-CAGCTCAGCCAATTCTTCAAT-3′; AIB1 probe, 6FAM-TGCCATGTGATACTCCAG AAG-Black Hole Quencher 1 (BHQ1); glyceraldehyde-3-phosphate dehydrogenase forward primer, 5′-CCCACATGGCCTCCAAGGAGTA-3′; glyceraldehyde-3-phosphate dehydrogenase reverse primer, 5′-GTGTACATGGCAACTGTGAGGAGG-3′; and glyceraldehyde-3-phosphate dehydrogenase probe, 6FAM-ACCCCTGGACCAGCCCCAGC-TAMRA.

cDNA Array Analysis. The method used to prepare samples for cDNA microarray analysis is outlined in the Affymetrix Gene Chip Expression Analysis Technical Manual, Section 2: Eukaryotic Sample and Array Processing. Total RNA was harvested from estrogen-stripped MCF-7 cells transfected with AIB1 or control siRNA for 48 hours (RNeasy Mini kit, Qiagen). Twenty micrograms of total RNA were used to synthesize double-stranded cDNA. T7 oligo(dT) primers [5′-GGCCAGTGAATTGTAATACGACTCACTATAGGGAGGCGG-$(dT)_{24}$-3′] were used to prime the first-strand cDNA synthesis. Synthesis of biotin-labeled cRNA from double-stranded cDNA was done with the Enzo BioArray High Yield RNA Transcript Labeling kit (Enzo Life Sciences, Farmingdale, NY). Twenty micrograms of fragmented biotin-labeled cRNA were hybridized to the Affymetrix Human Genome U133A GeneChip (Affymetrix, Santa Clara, CA). MCF-7 cells either transfected with the control or AIB1 siRNA were analyzed using four U133A chips.

Array Analysis. For each of the eight arrays, measurements from 22,283 genes were obtained. For each gene, an indicator of its expression level is given as either present, absent, or marginal call because it is assigned by Affymetrix Microarray suite software. Gene expression measurements that were <10 were given a threshold value of 10. Log base 2 transformations were applied to the gene expression values to reduce variation and to make the data

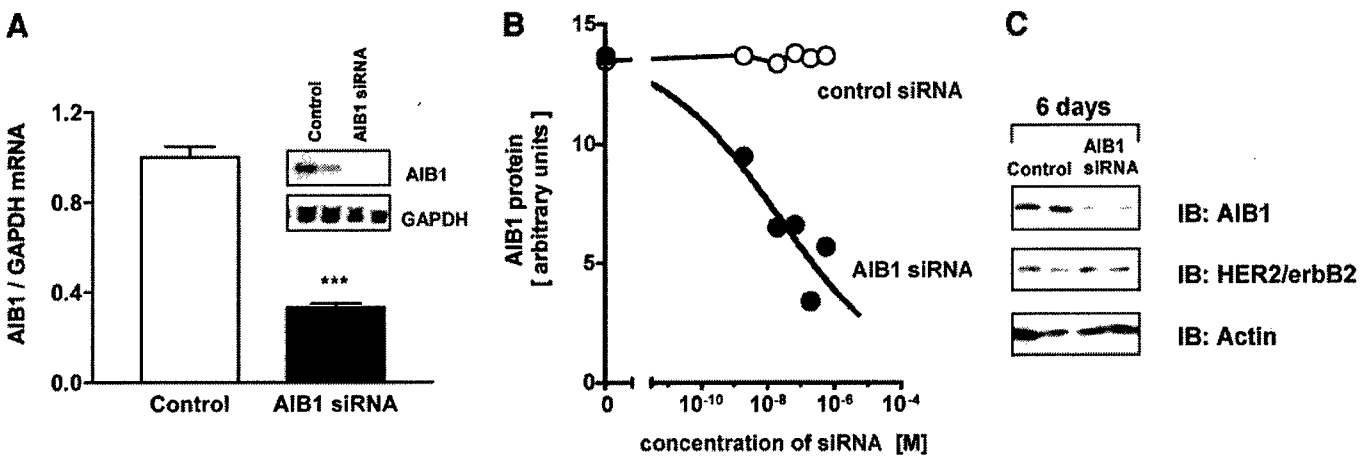

Fig. 1. The effect of AIB1 siRNA on endogenous AIB1 gene expression in MCF-7 cells. *A*. A 21-bp double-stranded RNA was designed against exon 7 of AIB1 mRNA. The control siRNA is also a 21-bp dsRNA but does not have any known homology to eukaryotic genes. The levels of AIB1 message after AIB1 siRNA transfection were examined by real time PCR and Northern blotting (*inset*). For real-time PCR analysis, total RNA was harvested from MCF-7 cells 48 hours after they were transfected with 2×10^{-7} mol/L AIB1 siRNA or control siRNA. Samples were run in duplicate and are normalized relative to glyceraldehyde-3-phosphate dehydrogenase (GAPDH). Cytoplasmic RNA was used for Northern blot analysis. To detect AIB1 mRNA, a 7.5-kb *Eco*RI fragment from pCMX-ACTR A38 (703–927 aa) was used as a probe. Quantitation of the Northern blotting was done with a phosphoimager and normalized relative to GAPDH. The graph represents the mean ± SE of four independent experiments. ***$P < 0.01$, Student's t test. *B*, concentration response of siRNA on AIB1 protein levels. Total cell lysates were harvested 48 hours after transfection and analyzed by Western blotting. AIB1 protein levels were quantitated by densitometry and normalized relative to β-actin. Nonlinear logistic regression analysis was used to determine the IC_{50}, 2×10^{-8} mol/L (± 7.8% SE). On the basis of this, 2×10^{-7} mol/L was the concentration of siRNA used in all subsequent experiments. *C*. AIB1 siRNA effectively knocks down protein expression up to 6 days after transfection of 2×10^{-7} mol/L AIB1 siRNA. No changes in the expression of both the HER2/erbB2 receptor and β-actin show that the siRNA specifically targets AIB1 protein and does not have nonspecific effects. Total cell lysates of were harvested 6 days after the transfection.

more normally distributed. Each gene that had an absent call from five or more of eight measurements was eliminated. This reduced the data set to 12,057 genes. The following analysis was done on the 12,057 genes with BRB-Array Tools (V.3.0.1). The intensity values were first normalized such that the median log intensity of each of the eight arrays is equal to the median log intensity for the reference array (BRB array tools arbitrarily choose the second array to be the reference array). Two sample t tests were carried out to compare the expression intensity between AIB1 high (control siRNA transfected) and AIB1 low (AIB1 siRNA transfected) arrays for each of the 12,057 genes with four arrays per group using the randomized variance model. A total of 124 genes showed a statistically significant difference between AIB1 high and AIB1 low at $P \leq 0.0025$ from the univariate test. The 124 genes include genes that were up or down-regulated by AIB1. The genes were also ranked according to P value.

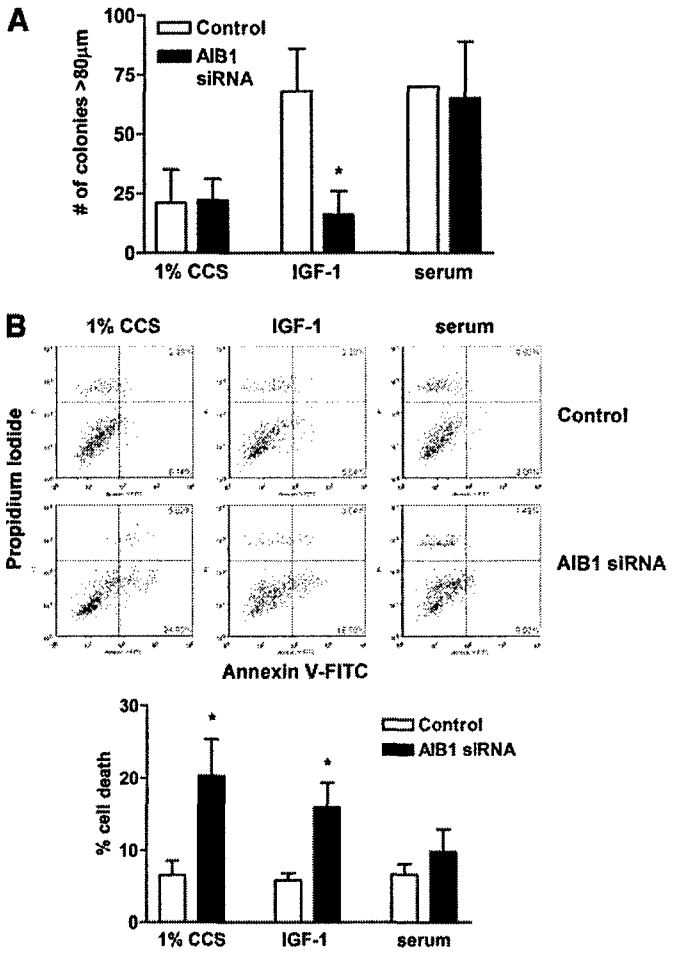

Fig. 2. AIB1 is critical for the growth and survival of MCF-7 cells under anchorage-independent conditions. *A*, soft agar colony formation of MCF-7 cells. A pool of MCF-7 cells was transfected with either AIB1 siRNA or control siRNA for 24 hours. The transfected cells were trypsinized, washed with IMEM +1% CCS, and plated in 0.35% soft agar dishes in the absence (1% CCS) or presence of 100 ng/mL IGF-I or 10% fetal bovine serum (serum). The colonies were measured after ~2 weeks. Colonies with a diameter ≥80 μm were counted with the Omnicon image analyzer. Experiments were carried out in triplicate. This graph is a representative figure out of three independent experiments. *Error bars* indicate SD. *, $P < 0.01$, relative to control siRNA sample. Student's t test. *B*, analysis of anoikis after AIB1 siRNA transfection. The cells were transfected with siRNAs as in *A*. After transfection, the cells were plated onto poly-HEMA–coated 60-mm dishes, a hydrogel that prevents cell attachment. The cells were treated with either 1% CCS, IGF-I or serum for 24 hours and harvested for apoptosis analysis by staining the cells with FITC-conjugated Annexin V and propidium iodide and performing a fluorescence-activated cell sorting analysis (Trevigen, Inc.). *Top panel:* cell death represents the total percentage of cells in early apoptosis (*bottom right quadrant* of the fluorescence-activated cell sorting analysis) and late apoptosis (*top right quadrant* of the FACS analysis). *Bottom panel:* the graph represents the mean ± SE of three independent experiments. *, $P < 0.01$, relative to control siRNA sample. Student's t test.

Table 1 *AIB1 siRNA effects on cell cycle progression of MCF-7 cells*

A. Cell cycle status of cells in suspension

	% (G_2 + S) phase	
Treatment	Control siRNA	AIB1 siRNA
1% CCS	25.5 (2.3)	23.1 (2.3)
IGF-I	33.2 (2.8)	31.9 (2.0)
Serum	32.2 (2.5)	28.5 (2.6)

B. Cell cycle status of attached cells

	% (G_2 + S) phase	
Treatment	Control siRNA	AIB1 siRNA
1% CCS	27.1 (0.6)	17.9 (4.4)
IGF-I	39.4 (3.6)	29.7 (5.8)
Serum	46.7 (4.4)*	41.6 (7.4)*

NOTE. Cell cycle analysis of suspended cells (A) and attached cells (B). MCF-7 cells were transfected with siRNA for 24 hours. Transfected cells were replated in poly-HEMA–coated (A) or –uncoated (B) 60-mm dishes and treated with 1% CCS and IGF-I or serum for 24 hours. Cells were then harvested and stained with the Vindelov method to determine the percentage of cells in each phase of the cell cycle. The percentage represents the mean (SD) of two independent experiments done in duplicate. An ANOVA analysis was done for control and AIB1 siRNA conditions and for suspension growth and attached cells. A significant difference (*, $P < 0.05$) was only found for serum stimulation relative to 1% CCS.

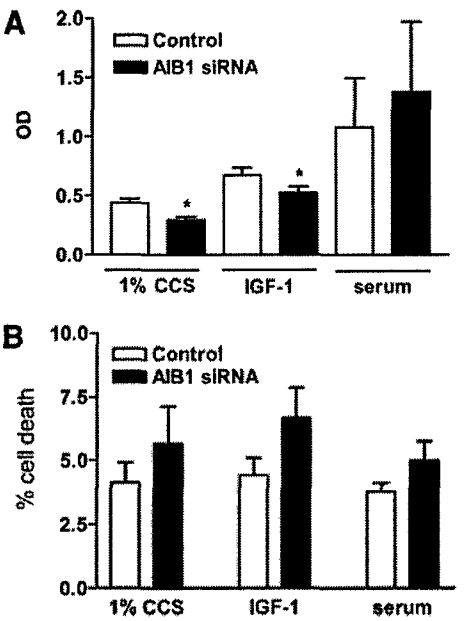

Fig. 3. Reduction of AIB1 decreases the rate of anchorage-dependent proliferation without significant changes in the levels of cell death. *A*, reduction in basal rate of proliferation: MCF-7 cells were transiently transfected with AIB1 siRNA or control siRNA for 24 hours. A total of 4500 cells was placed into each well of a 96-well plate and treated with 1% CCS, IGF-I, or serum. Cell growth was measured by the WST-1 colorimetric assay up to 8 days. Each experiment was done in triplicate. The graphs represent the mean ± SE of three independent experiments. *, $P < 0.05$, Student's t test. *B*, cell death in attached conditions: 24 hours after siRNA transfection, cells were replated in 60-mm dishes and treated with 1% CCS, IGF-I, and serum. After 24 hours, the cells were harvested and examined for percentage of cells in early and late apoptosis by Annexin V staining (Trevigen, Inc.). The graph represents the mean ± SE of three independent experiments. There is no significant difference between the results at $P < 0.05$. Student's t test.

RESULTS

Effect of siRNA on AIB1 Gene Expression. To study the role of AIB1 in IGF-I signaling, we used siRNA directed at nucleotides 564–582 of AIB1 to selectively reduce AIB1 gene expression in the MCF-7 breast cancer cell line. This region bears no significant homology to other coactivators or sequences in the human genome database. The AIB1 siRNA reduced the AIB1 mRNA (Fig. 1*A*) and AIB1 protein in a concentration-dependent fashion (Fig. 1*B*). The

Table 2 *Entire list of altered genes from the cDNA array analysis of AIB1 high (control) versus AIB1 low (AIB1 siRNA)*

	Probe set	Mean expression for AIB1 high	Mean expression for AIB1 low	Fold (AIB high/AIB low)	Up (+) or down (−) regulated by AIB1	Rank of *P* of the randomized variance test	*P* of the randomized variance test
RAB, member of RAS oncogene family-like 4	205037 at	274.876	654.179	0.42	−	1	0.00002
Malic enzyme 1, NADP(+)-dependent, cytosolic	204058 at	440.668	1044.197	0.422	−	2	0.0000242
p53-induced protein PIGPC-1	217744 s at	571.677	1195.691	0.478	−	3	0.0000321
AIB1	209062 x at	1682.874	726.757	2.316	+	4	0.0000377
Cyclin D1	208712 at	3262.634	1292.907	2.523	+	5	0.0000426
Hypothetical protein FLJ10842	222132 s at	666.67	297.556	2.24	+	6	0.0000501
RAB27B, member RAS oncogene family	207017 at	44.51	111.832	0.398	−	7	0.0000511
Sialyltransferase 8D (α-2, 8-polysialytransferase)	206925 at	109.627	318.894	0.344	−	8	0.0000721
Chromagranin A (parathyroid secretory protein 1)	204697 s at	598.087	242.007	2.471	+	9	0.0000778
Chemokine (C-X-C motif) ligand 12 (stromal cell-derived factor 1)	203666 at	551.907	258.868	2.132	+	10	0.000082
Histone 1, H2bd	222067 x at	1273.525	4863.035	0.262	−	11	0.0000901
AIB1	209060 x at	2886.879	1409.345	2.048	+	12	0.0000974
3′-Phosphoadenosine 5′-phosphosulfate synthase 2	203058 s at	81.223	179.569	0.452	−	13	0.0001073
	203231 s at	78.312	276.067	0.284	−	14	0.000118
Pirin	207469 s at	198.894	669.774	0.297	−	15	0.0001229
Hypothetical protein FLJ10842	211352 s at	2164.567	1043.125	2.075	+	16	0.0001234
PHD finger protein 10	221786 at	1404.191	697.794	2.012	+	17	0.0001291
Bone morphogenetic protein 7 (osteogenic protein 1)	211259 s at	307.814	140.98	2.183	+	18	0.0001298
Hypothetical protein FLJ10842	218568 at	399.582	190.925	2.093	+	19	0.0001303
MAPK-1	212271 at	1279.667	569.648	2.246	+	20	0.0001316
	203232 s at	132.079	312.431	0.423	−	21	0.0001405
Chromosome 6 open reading frame 56	204048 s at	541.053	1017.398	0.532	−	22	0.0001614
3′-Phosphoadenosine 5′-phosphosulfate synthase 2	203060 s at	125.006	297.243	0.421	−	23	0.0001616
Hypothetical protein MGC2963	221255 s at	836.521	1710.86	0.489	−	24	0.000166
PDZ-1 domain-containing 1	205380 at	699.117	211.344	3.308	+	25	0.0001706
PHD finger protein 10	221787 at	936.315	458.354	2.043	+	26	0.0001719
Karyopherin α 1 (importin α 5)	202056 at	424.574	181.884	2.334	+	27	0.0001824
Karyopherin α 1 (importin α 5)	202055 at	959.842	391.313	2.453	+	28	0.0001887
MHC class I polypeptide-related sequence B	206247 at	667.084	308.834	2.16	+	29	0.0001928
Sapiens cDNA FLJ20338 fis, clone HEP 12179	214079 at	1694.251	329.078	5.148	+	30	0.0001957
Molybdenum cofactor synthesis 2	218212 s at	1431.594	624.03	2.294	+	31	0.0002208
HMBA-inducible	202814 s at	528.328	934.206	0.566	−	32	0.0002883
Filamin B	208613 s at	823.305	389.677	2.113	+	33	0.0002931
Pleckstrin homology domain containing, family B (evectins) member 2	201411 s at	517.485	1117.563	0.463	−	34	0.000316
Kynureninase (L-lynurenine hydrolase)	217388 s at	277.552	626.48	0.443	−	35	0.0003291
Potassium channel, subfamily K, member 5	219615 s at	566.977	259.781	2.183	+	36	0.0003647
Methionyl aminopeptidase 2	202015 x at	27.966	59.198	0.472	−	37	0.0003691
Glyoxalase I	200681 at	5937.301	2780.38	2.135	+	38	0.0003918
S100 calcium binding protein A14	218677 at	1140.565	2211.092	0.516	−	39	0.0003937
Olfactomedin 1	213131 at	1061.422	570.195	1.862	+	40	0.0004057
Polymerase (RNA) II (DNA-directed) polypeptide D	214144 at	146.593	254.863	0.575	−	41	0.0004117
Butyrophilin, subfamily 3, member A3	38241 at	67.413	177.872	0.379	−	42	0.0004601
WW domain binding protein 11	217821 s at	293.572	492.855	0.596	−	43	0.0004607
Hydroxy prostaglandin dehydrogenase 15-(NAD)	211548 s at	244.116	100.061	2.44	+	44	0.0004619
Synaptotagmin I	203998 s at	133.708	249.236	0.536	−	45	0.0004762
Chromosome 6 open reading frame 56	204049 s at	588.212	1310.993	0.449	−	46	0.0005077
DICER-1	213229 at	2307.863	1114.54	2.071	+	47	0.000515
Dodecenoyl-Coenzyme A δ isomerase (3,2 trans-enoyl-Coenzyme A isomerase)	209759 s at	653.268	1380.144	0.473	−	48	0.0005196
RAB 15, member RAS oncogene family	59697 at	1070.718	574.105	1.865	+	49	0.0005535
Solute carrier family 25 (mitochondrial carrier; ornithine transporter) member 15	218653 at	823.559	404.301	2.037	+	50	0.0005662
Ectonucleoside triphosphoate diphosphohydrolase 1	207691 x at	145.162	271.393	0.535	−	51	0.0005858
DICER-1	212888 at	1579.524	687.527	2.297	+	52	0.00062
Zinc finger, DHHC domain containing 3	218078 s at	515.903	307.607	1.677	+	53	0.0006223
Cdc42 guanine nucleotide exchange factor (GEF) 9	203264 s at	41.278	101.05	0.408	−	54	0.0006257
Trophoblast-derived noncoading RNA	214657 s at	378.673	934.216	0.405	−	55	0.0006377
KIAA0657 protein	212776 s at	1433.679	769.539	1.863	+	56	0.0007141
Phospholipase A2, group XII	221027 s at	258.746	549.612	0.471	−	57	0.0007233
Solute carrier family 7 (cationic amino acid transporter, y_system), member 5	201195 s at	6410.213	2766.12	2.317	+	58	0.0007245
Sialyltransferase	204542 at	230.423	442.079	0.521	−	59	0.0007661
Lin-7 homology A (*C. elegans*)	206440 at	232.047	447.247	0.519	−	60	0.000769
Family with sequence similarity 16, member A, X linked	203974 at	933.932	388.651	2.403	+	61	0.0007798
	220033 at	123.138	200.674	0.614	−	62	0.0007865
	217403 s at	70.891	135.505	0.523	−	63	0.0008073
Golgi autoantigen, golgin subfamily a, 2	204384 at	250.411	536.387	0.467	−	64	0.0008243
Abhydrolase domain-containing 3	213017 at	300.266	612.578	0.49	−	65	0.0008298
Palmitoyl-protein thioesterase 1 (ceroid-lipofuscinosis, neuronal 1, infantile)	200975 at	2632.758	5182.401	0.508	−	66	0.0008407
Keratin 8	209008 x at	19559.105	10904.508	1.794	+	67	0.0008456
Sorting nexin 5	217792 at	1105.939	615.404	1.797	+	68	0.0008456
Translocase of outer mitochondrial membrane 22 homologue (yeast)	217960 s at	315.36	675.567	0.467	−	69	0.0008724
ATP-binding cassette, sub-family C (CFTR/MRP), member 3	208161 s at	253.505	697.4	0.364	−	70	0.0009091
Golgi phosphoprotein 2	217771 at	334.384	162.16	2.062	+	71	0.0009642

Table 2 *Continued*

	Probe set	Mean expression for AIB1 high	Mean expression for AIB1 low	Fold (AIB high/AIB low)	Up (+) or down (−) regulated by AIB1	Rank of *P* of the randomized variance test	*P* of the randomized variance test
Deiodinase, iodothyronine, type I	206457 s at	72.876	139.655	0.522	−	72	0.0009778
Solute carrier family 9 (sodium/hydrogen exchange), isoform 3 regulatory factor 1	201349 at	5586.867	3087.018	1.81	+	73	0.0009937
Sarcoma antigen	220793 at	180.675	351.721	0.514	−	74	0.0010088
Toll-like receptor 3	206271 at	103.563	186.645	0.555	−	75	0.0010269
Karyopherin α 1 (importin α 5)	202058 s at	434.526	260.88	1.666	+	76	0.0010678
Inhibin, β B (activin AB neta polypeptide)	205258 at	1782.915	1014.699	1.757	+	77	0.0011023
Damage-specific DNA binding protein 2, 48 kDA	203409 at	317.875	547.097	0.581	−	78	0.0011139
Spastic ataxia of Charlevoix-Saguenay (sacsin)	213262 at	46.648	23.442	1.99	+	79	0.0011206
Bone morphogenetic protein 7 (osteogenic protein 1)	209590 at	1062.787	584.447	1.818	+	80	0.0011361
Myristoylated alanine-rich protein kinase C substrate	201669 s at	656.271	1391.009	0.472	−	81	0.001137
Histone deacetylase 1	201209 at	1258.795	2076.041	0.606	−	82	0.00117
MHC class I region ORF	206082 at	178.538	377.635	0.473	−	83	0.0011727
Phosphodiesterase 4A, cAMP-specific (phosphodiesterase E2 dunc homologue, Drosophila)	204735 at	212.51	121.629	1.747	+	84	0.001249
Inhibin α	210141 s at	475.26	212.213	2.24	+	85	0.0012506
TP53 target gene 1	209917 s at	278.896	739.962	0.377	−	86	0.0012653
Spermatogenesis-associated 2	204434 at	402.499	247.275	1.628	+	87	0.0012892
Insulin-induced gene 1	201626 at	1384.879	2681.165	0.517	−	88	0.0013424
Serum/glucocorticoid regulated kinase-like	220038 at	187.597	84.055	2.232	+	89	0.001394
Hypothetical protein LOC90333	214751 at	132.651	281.339	0.471	−	90	0.0014372
MRS2-like, magnesium homeostasis factor (*S. cerevisiae*)	218536 at	433.963	241.151	1.8	+	91	0.0014565
WNT inhibitory factor 1	204712 at	21.107	63.23	0.334	−	92	0.0014629
Polymerase (DNA directed) θ	219510 at	315.331	154.606	2.04	+	93	0.0014656
Ectonucleoside triphosphoate diphosphohydrolase 1	209474 s at	91.312	181.342	0.504	−	94	0.0015323
DKFZP586O0120 protein	201863 at	1066.931	2047.963	0.521	−	95	0.0015545
Cyclin D1	203003 at	71.257	27.906	2.553	+	96	0.0015729
Mouse mammary tumor virus receptor homologue 1	212484 at	1121.985	613.647	1.828	+	97	0.0016537
α Glucosidase II α subunit	211934 x at	853.545	1802.795	0.473	−	98	0.001746
Coiled-coil protein BICD2	213154 s at	356.548	616.454	0.578	−	99	0.0018189
KIAA0657 protein	212775 at	1599.555	879.879	1.818	+	100	0.001845
Bcl-2	207005 s at	104.988	26.786	3.92	+	101	0.0018496
Hypothetical protein DKFZp434G2311	212712 at	550.83	331.554	1.661	+	102	0.0018503
Phosphoenolpyruvate carboxykinase 2 (mitochondrial)	202847 at	897.913	1530.352	0.587	−	103	0.0018568
Aldehyde oxidase 1	205082 s at	92.882	316.055	0.294	−	104	0.001889
KIAA0515	212069 s at	807.408	445.35	1.813	+	105	0.0019455
UDP-GlcNAc:betaGal β-1,3,-N-acetylglucosaminoyltransferase 6	203188 at	875.021	555.977	1.574	+	106	0.0019878
Platelet-derived growth factor receptor-like	205226 at	88.627	137.983	0.642	−	107	0.002008
c-src tyrosine kinase	202329 at	619.421	1025.285	0.604	−	108	0.0020142
Golgi autoantigen, golgin subfamily a, 2	35436 at	467.131	849.159	0.55	−	109	0.0020245
Acidic (leucine-rich) nuclear phosphoprotein 32 family, member A	201051 at	2169.058	1210.09	1.792	+	110	0.0020493
Hydroxy prostaglandin dehyrogenase 15-(NAD)	211549 s at	150.119	85.033	1.765	+	111	0.0021083
Hydroxy prostaglandin dehyrogenase 15-(NAD)	203914 x at	308.595	152.825	2.019	+	112	0.0021965
Butyrophilin, subfamily 3, member A3	204821 at	58.168	184.976	0.314	−	113	0.0022086
Galactokinase 2	205219 s at	240.849	388.952	0.619	−	114	0.0022089
Frequently rearranged in advanced T-cell lymphomas 2	209864 at	606.599	1012.928	0.599	−	115	0.0022226
Caldesmon 1	205525 at	29.357	46.41	0.633	−	116	0.0022346
Hydroxy prostaglandin dehydrogenase 15-(NAD)	203913 s at	255.449	117.952	2.166	+	117	0.0022542
Proteasome (prosome, macropain) subunit, β type, 8 (large multifunctional protease 7)	209040 s at	213.011	708.401	0.301	−	118	0.0023201
F-box and leucine-rich repeat protein 11	208988 at	544.302	942.391	0.578	−	119	0.0023575
Tara-like protein	210276 s at	268.181	592.816	0.452	−	120	0.002376
Myristoylated alanine-rich protein kinase C substrate	201670 s at	251.389	422.842	0.595	−	121	0.002406
Testis expressed sequence 27	218020 s at	1470.697	941.449	1.562	+	122	0.0024394
Suppression of tumorigenicity 7	207871 s at	128.766	226.667	0.568	−	123	0.0024562
Hemoglobin α 2	209458 x at	890.865	398.769	2.234	+	124	0.002482

siRNA concentration used in our experiments, 2×10^{-7} mol/L, produced a >80% reduction in cellular AIB1 protein levels (Fig. 1*B*). In addition, after a single transfection of siRNA, we found that the AIB1 protein levels were still repressed after 6 days (Fig. 1*C*). A control-scrambled sequence siRNA had no effect on AIB1 gene expression (Fig. 1*A–C*). The expression of a number of unrelated proteins such as actin or HER2 was unaltered by either siRNA. Thus, application of AIB1-directed siRNA was an effective and selective method of long-term suppression of endogenous AIB1 levels, enabling experiments to determine the impact of reducing endogenous AIB1 on MCF-7 cells.

Effect of Reduction of Endogenous AIB1 on Anchorage-independent Growth of MCF-7 Cells. An important growth factor induced phenotypic change, and a hallmark of malignant transformation is the ability of cells to form colonies in soft agar. This anchorage-independent growth involves cell cycle regulatory genes, as well as genes that prevent apoptosis under anchorage-independent conditions (*i.e.,* anoikis). IGF-I has been reported as a powerful inducer of anchorage-independent growth in MCF-7 breast cancer cells, and we first determined if AIB1 played a role in this IGF-I effect. IGF-I induced a 3-fold increase in the number of MCF-7 colonies formed, and this increase was completely negated by treatment with AIB1 siRNA (Fig. 2*A*). In contrast, a similar 3-fold increase in colony formation observed with serum treatment was unaffected by the reduction of AIB1 (Fig. 2*A*), suggesting a selective role of AIB1. In 1% CCS, the colony count is indistinguishable from the baseline of this assay, and this is unaffected by AIB1 siRNA treatment. The effects of AIB1 siRNA on IGF-I–induced colony formation were not

due to nonspecific activation of RNA degradation because parallel experiments in which endogenous AIB1 were reduced by the expression of tetracycline-regulated ribozymes (14) showed the same selective inhibition of IGF-I–induced colony formation (data not shown).

Increases in colony formation in anchorage-independent growth due to growth factor stimulation result from a balance between increased numbers of cells entering the cell cycle and reduction in anoikis. Therefore, it was of interest to determine which of these processes was affected by the reduction of AIB1. To examine this, we grew MCF-7 cells on poly-HEMA–coated dishes that prevent attachment and forces the cells to grow anchorage independently (24). Fluorescence-activated cell sorting analysis showed that reduction of AIB1 levels had no significant effect on progression of the cells into G_2 + S either under basal, IGF-I, or serum-induced growth conditions (Table 1*A*). Annexin V staining to quantitate apoptosis, however, showed that IGF-I was unable to rescue the cells with reduced AIB1 levels from anoikis, whereas the rescue by serum was unaffected (Fig. 2*B*). The increase in anoikis in 1% CCS in the presence of AIB1 siRNA did not register in the soft agar colony count because this was already at background levels of this latter assay in the absence of AIB1 siRNA treatment and is therefore not sensitive to additional reductions. Thus, there are no factors in 1% CCS that stimulate colony formation, but AIB1 siRNA can still cause apoptosis in these cells because there are no factors in 1% CCS to rescue them. Overall, the results suggest that IGF-I–induced survival of cells growing in suspension depends on an AIB1-dependent signaling pathway, whereas serum does not.

AIB1 Effects on Anchorage-dependent Growth. To determine whether the effect of AIB1 siRNA were unique to anchorage-independent growth conditions, we also determined its effects under anchorage-dependent growth conditions. Attached cells show a reduced growth rate (~30%) after reduction of AIB1 and the stimulation by IGF-I (1.7-fold) or by serum (2.8-fold) was not affected by reduced AIB1 levels. These data imply that cell attachment can circumvent the rate-limiting signal pathways required for IGF-I–dependent survival of cells in suspension (Fig. 3*A*). Interestingly, AIB1 siRNA treatment reduced by 34% the number of MCF-7 cells in G_2 + S phases of the cell cycle (Table 1*B*), which explains the reduction of the overall growth rate independent of exogenously added growth stimulus. Under attached growth conditions, there was a trend to increased apoptosis with reduction in AIB1 with siRNA, but the differences were not statistically significant (Fig. 3*B*). In the MCF-7 Rz29 cell lines (14), similar results were also obtained (data not shown).

Analysis of Genes Whose Expression Is Dependent on AIB1. To determine genes that might be critical targets of AIB1 during proliferative responses in MCF-7 cells, we compared gene array analysis of MCF-7 cells after treatment with AIB1 or control siRNA for 2 days. The Affymetrix U133A human gene chip that represents 33,568 transcripts was used to evaluate gene expression profiles under these different conditions, and we found 124 genes that showed a statistically significant difference between AIB1 high (control siRNA transfected) and AIB1 low (AIB1 siRNA transfected) at $P \leq 0.0025$ (Table 2). Interestingly, several genes that are known to be critical for cell cycle regulation, anoikis, and apoptosis, notably cyclin D1, Bcl-2, and MAPK [extracellular signal-regulated kinase (ERK) 1/2] were highly dependent on AIB1 levels for their sustained expression (highlighted in Table 2). In our array analysis, we also found that the expression of a number of genes was up-regulated by reducing AIB1 with siRNA (Table 2), indicating that high AIB1 levels normally suppress expression of these genes.

In a separate set of array analyses, we also examined the effect of a short-term 1 hour treatment by IGF-I on gene expression after treatment of MCF-7 cells with AIB1 siRNA and control siRNA. This was to determine whether there were critical immediate early genes that IGF-I–regulated dependent on the AIB1 levels. However, at $P \leq 0.0025$, this analysis did not differ significantly from the AIB1 siRNA *versus* control siRNA analysis. Thus, 1 hour of IGF-I treatment after pretreatment with AIB1 siRNA did not alter gene expression in comparison to cells pretreated with AIB1 siRNA alone (this comparison is not shown).

To assess whether altered mRNA expression due to AIB1 reduction was also reflected at the protein level, we did a series of Western blot analysis for those proteins known to be crucial for cell growth and survival. The protein levels of cyclin D1, Bcl-2, and ERK2 (but not ERK1) were reduced (90, 40, and 40%, respectively) by lowering the AIB1 levels by >90% in attached MCF-7 cells (Fig. 4). AIB1 siRNA reductions in expression of these genes were also observed in the presence of IGF-I (Fig. 4). IGF-I clearly induced the expression of cyclin D1 (4-fold) and caused a smaller 1.7-fold increase in the protein expression of ERK2 (Fig. 4). The basal levels of both cyclin D1 and Bcl-2 were increased under anchorage-independent conditions (Fig. 4), and IGF-I did not increase these levels any further (Fig. 4). Overall, it is clear that in basal or IGF-I–treated conditions or in cells attached or in suspension, targeting of AIB1 was effective in producing decreases in cyclin D1, Bcl-2, and ERK2 protein levels. Maintenance of the expression of these genes by AIB1 could be involved in both basal and IGF-I–induced growth responses in MCF-7 cells.

AIB1 Is Required to Maintain Expression of Molecules Critical to Insulin-like Growth Factor I Signaling. A somewhat surprising aspect of our cDNA array analyses was that after 48 hours of exposure to AIB1 siRNA, we did not see significant changes in the mRNA levels of molecules that specifically transmit IGF-I signaling such as the IGF-IR, IRS-1, IRS-2, or IGF-binding protein family members. We had conjectured that changes in the expression of these molecules after reduction of AIB1 might explain the selective effect on IGF-I but not serum signaling, and thus, we next determined the impact of the reduction of AIB1 on the protein levels of IGF-I–signaling molecules to pick up potential posttranscriptional effects. We did Western blot analysis of IGF-I–signaling molecules in the presence of control or AIB1 siRNA in both attached and suspension growth (Fig. 5, left and right panels). Under the anchorage-independent conditions, which had revealed the dependence of IGF-I survival signals on AIB1 (see

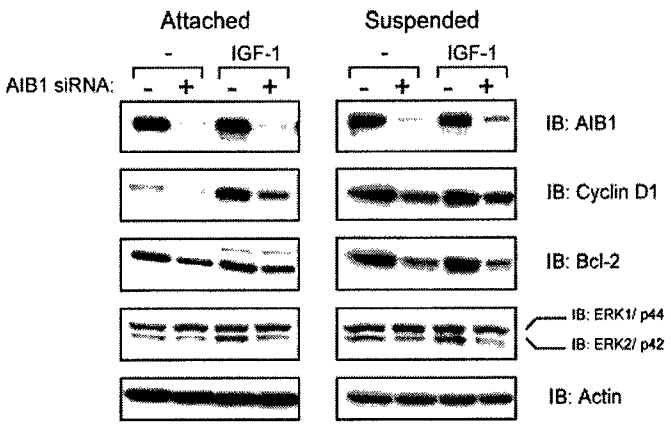

Fig. 4. Changes in protein expression of critical genes involved in proliferation, cell cycle, and apoptosis after AIB1 siRNA treatment. For attached cells, estrogen-stripped MCF-7 cells were transfected with control or AIB1 siRNA and treated with or without IGF-I in the presence of 1% CCS. Whole cell lysates were harvested after 48 hours and analyzed by Western blot analysis. In suspension growth conditions, cells were transfected for 18 to 24 hours with siRNA and replated in poly-HEMA (10 μg/mL)–coated dishes for another 24 hours before whole cell lysates were harvested and analyzed by Western blot analysis. Data in Fig. 6 are from the same experiment as Fig. 4. Blots are representative results from three independent experiments.

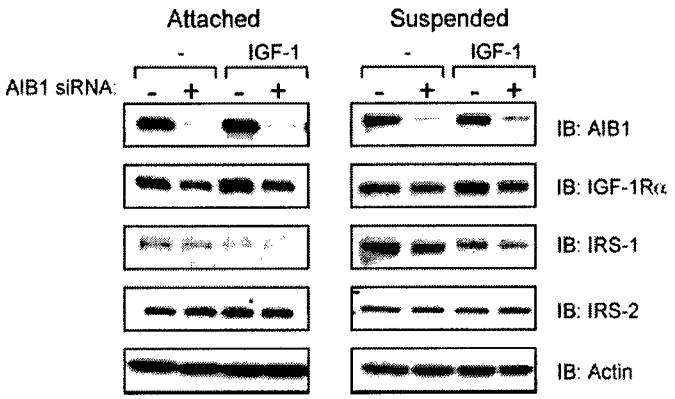

Fig. 5. AIB1 has a role in regulating some members of the IGF-I–signaling pathway. For attached cells, estrogen-stripped MCF-7 cells were transfected with control or AIB1 siRNA and treated with or without IGF-I in the presence of 1% CCS. Whole cell lysates were harvested after 48 hours and analyzed by Western blot analysis. In suspension growth conditions, cells were transfected for 18 to 24 hours with siRNA and replated in poly-HEMA (10 μg/mL)–coated dishes for another 24 hours before whole cell lysates were harvested and analyzed by Western blot analysis. Blots are representative results from three experiments.

Fig. 2), we found that IGF-I receptor protein levels were reduced by 50% upon reduction of AIB1. Furthermore, we also observed a smaller 10 to 20% reduction in IRS-1 protein levels in the presence of IGF-I (Fig. 5*A*, right panel). IRS-2 protein was not altered. IGF-IR levels in attached cells showed a similar reduction of the IGF-I receptor protein after AIB1 siRNA treatment and no detectable alteration in IRS-1 or IRS-2 proteins (Fig. 5, left panel). Thus, we conclude that the IGF-I receptor is dependent on AIB1 for its protein expression levels in MCF-7 cells. This regulation appears to be mediated at the posttranscriptional level because we did not detect significant changes in the IGF-IR mRNA levels on the cDNA array analysis.

AIB1 Is Required for Estrogen-dependent and -independent Regulation of Gene Expression in MCF-7 Cells. We have determined previously that AIB1 plays a rate-limiting role in the estrogen-induced proliferation of MCF-7 cells (14). There is much evidence for cross-talk between the IGF-I and ER-signaling pathways (25–27) and the expression of IGF-1R, IRS-1, cyclin D1, Bcl-2, and MAPK are all regulated by estrogen (28–33). We therefore hypothesized that some if not all of the effects that we saw on gene expression by reducing cellular levels of AIB1 might be mediated through a reduction in ER signaling. Interestingly, we found that the expression of ER-α itself was not reduced under basal conditions after AIB1 siRNA treatment under attached conditions (Fig. 6*A*). However, in suspension conditions, we observed a decrease in ER levels in the presence of AIB1 siRNA. Thus, it was possible that the ER reduction alone could explain some of the effects of AIB1 siRNA in suspension. To examine the role of estrogen in the gene expression changes that we observed in the presence of AIB1 siRNA, we repeated the analysis of protein expression changes in the presence of the antiestrogen ICI 182,720 (ICI, Faslodex), which blocks estrogen binding to the receptor, as well as down-regulates the ER levels (Fig. 6*A*, right panel; ref. 34). We argued that if the effects of AIB1 were dependent on ER, then in the presence of antiestrogen, we would no longer see the AIB1 siRNA effect. Interestingly, AIB1 siRNA-dependent reductions in cyclin D1, Bcl-2, and ERK2 that we had observed in Fig. 4 were all preserved in the presence of ICI under attached conditions (Fig. 6*B*). However, the basal reduction in cyclin D1 was only 30% compared with the >80% reduction that we saw in the absence of ICI. This suggests that a large portion of the basal expression of cyclin D1 is maintained through estrogen signaling. In contrast, the magnitude of the AIB1 siRNA reduction in Bcl-2 and ERK2 were comparable in the presence or absence of antiestrogen. Although the IGF-IR is known to be an estrogen-induced gene, AIB1 siRNA treatment was still able to decrease IGF-IR expression irrespective of ICI (compare Fig. 5 with Fig. 6*B*). Overall, this data indicates that a large portion of the basal and IGF-I–induced changes in gene expression that we observed that were dependent on AIB1 were occurring independent of ER signaling.

AIB1 Is Required for IGF-I Signaling and Phenotypic Changes in the MDA MB-231 Breast Cancer Cell Line. To determine whether the dependence of IGF-I signaling was observed in other breast cancer cell lines, we examined the effect of AIB1 siRNA on the human breast cancer cell line, MDA MB-231. These cells are ER negative and proliferate in response to IGF-I (28). To determine whether similar genes were involved in the AIB1 effect in these cells as MCF-7 cells, we did immunoblot analysis of cell cycle and apoptosis genes, as well as for molecules involved specifically in IGF-I signaling. Similar to MCF-7 cells, cyclin D1 and ERK2 gene expression were dependent on maintaining high AIB1 levels (Fig. 7*A*). However, Bcl-2 levels were unaffected by AIB1 siRNA treatment. Unlike MCF-7 cells, none of these genes were induced by IGF-I in the MDA MB-231 cells (Fig. 7*A*). Interestingly, in MCF-7 cells, we observed that IGF-IR and to a certain extent IRS-1 expression were dependent on AIB1, but in MDA MB-231 cells, no changes in the expression of any of these proteins was observed (Fig. 7*B*).

The Role of AIB1 in IGF-I–induced Phosphatidylinositol 3′-Kinase (PI3k) and MAPK Signaling in Breast Cancer Cells. The data thus far indicated that neither the estrogenic effects nor the regulation of IGF-I–signaling molecules was the principal mechanism whereby AIB1 specifically effected IGF-I signaling. We therefore sought to de-

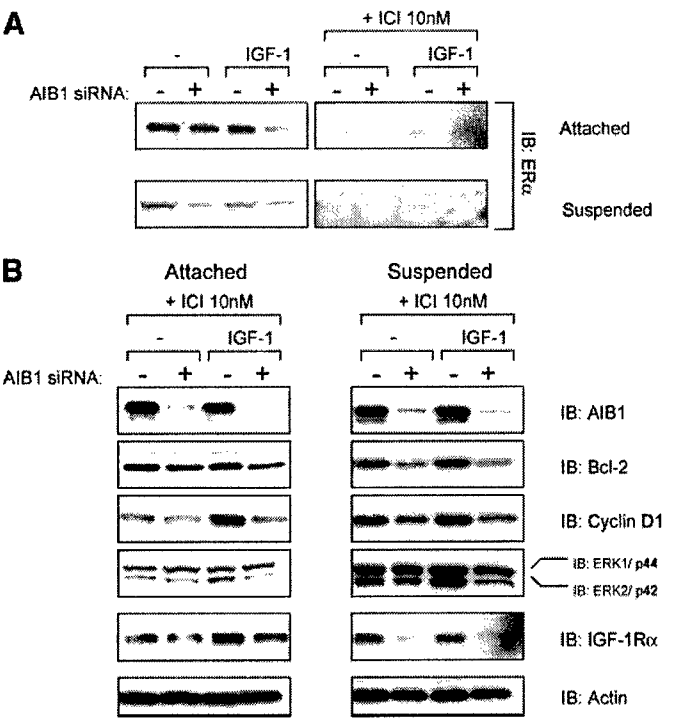

Fig. 6. The ability of AIB1 to regulate the expression of Bcl-2, cyclin D1, IGF-IR, and MAPK in the presence of IGF-I is independent of estrogen signaling. *A* and *B*. In attached growth conditions, estrogen-stripped MCF-7 cells were transfected with control or AIB1 siRNA and treated with or without IGF-I in the presence of 1% CCS and 10 nmol/L ICI. Whole cell lysates were harvested after 48 hours. In suspension growth conditions, cells were transfected for 18 to 24 hours with siRNA and replated in poly-HEMA (10 μg/mL)–coated dishes for another 24 hours before whole cell lysates were harvested. Lysates were analyzed by Western blot analysis with antibody probes as indicated. Data in Fig. 6 are from the same experiment as Fig. 4. Blots are representative results from three experiments.

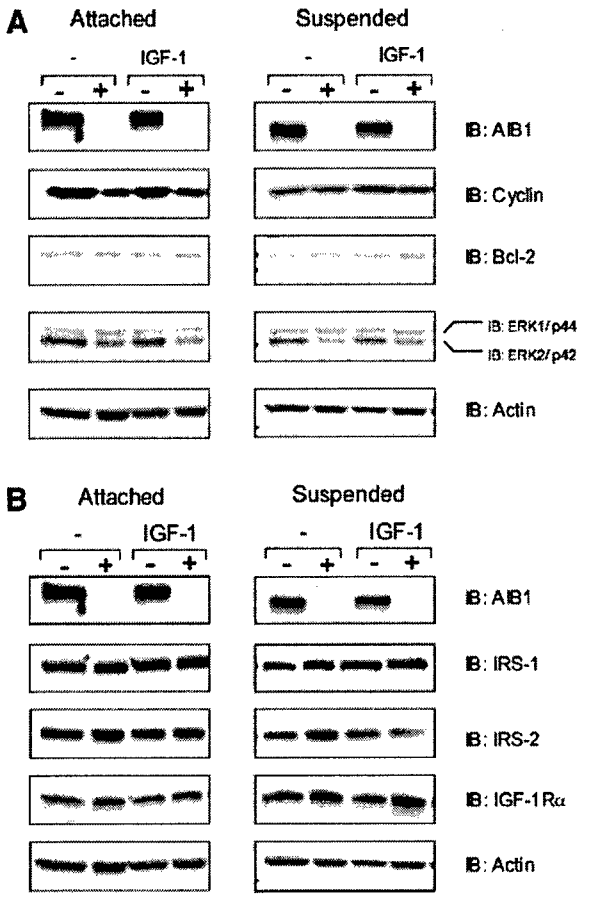

Fig. 7. Reduction of AIB1 in an ER-α–negative breast cancer cell line, MDA MB-231, regulates the expression of cyclin D1. *A* and *B*. In attached growth conditions, MDA MB-231 cells were transfected with control or AIB1 siRNA and treated with or without IGF-I in the presence of 1% CCS. Whole cell lysates were harvested after 48 hours. In suspension growth conditions, cells were transfected for 18 to 24 hours with siRNA and replated in poly-HEMA (10 μg/mL)–coated dishes for another 24 hours before whole cell lysates were harvested. Lysates were analyzed by Western blot analysis with antibodies as indicated. Blots are representative results from two experiments.

termine whether down-regulation of AIB1 directly affected activation of IGF-I–signaling pathways. For these experiments, we pretreated MCF-7 or MDA MB-231 cells (attached or suspended) for 48 hours with AIB1 siRNA and then determined the responsiveness of the cells to short-term treatment with IGF-I (0 to 30 minutes; Fig. 8). We examined the levels of AKT and its phosphorylation status on Ser^{473} as a readout of the sensitivity of the PI3k pathway and measured ERK 1/2 levels and their phosphorylation as a read out of MAPK activation. In attached conditions, in both MCF-7 and MDA MB-231 cells, we observed a reduction in the ratio of phospho-AKT to AKT, indicating a decreased sensitivity of the PI3k pathway to IGF-I (Fig. 8, *A* and *B*). However, the reduction in MCF-7 cells was less than that observed in MDA MB-231 cells, and the reduction in the phospho-AKT to AKT ratio was primarily due to an increase in AKT levels rather than a reduction in phosphorylation of AKT (Fig. 8*A*). Under suspension conditions (equivalent to the soft agar colony formation conditions) the IGF-I–induced changes in phospho-AKT to AKT ratio are unaltered in MCF-7 cells by AIB1 siRNA treatment, but the ratio was still reduced in MDA MB-231 cells (Fig. 8, *C* and *D*).

In contrast to the changes in AKT activation under all conditions and in both cell lines, treatment with AIB1 siRNA did not change the time course or the magnitude of ERK 1/2 phosphorylation after IGF-I stimulation (Fig. 8*A–D*). Overall, these data indicate that AIB1 levels determine the sensitivity of the PI3k pathway to IGF-I signaling in these breast cancer cell lines under certain plating conditions, but changes in AIB1 levels appear to have little effect on MAPK signaling.

DISCUSSION

The role of AIB1 and other coactivators in nuclear receptor signaling is well established. In this study, we now show that AIB1 can also be rate-limiting for IGF-I–stimulated growth of MCF-7 human breast tumor cells. This is consistent with the finding in p/CIP (AIB1 mouse homologue)-knockout mice that IGF-I stimulation of proliferation of mouse embryonic fibroblast cells was significantly reduced by deletion of p/CIP (18). However, in contrast to Wang *et al.* (18), where only a few changes in gene expression were observed upon array analysis of $pCIP^{-/-}$ *versus* wild-type mouse embryonic fibroblast cells, in MCF-7 cells, a number of critical signaling molecules were dependent on AIB1 for their expression and regulation. Most significantly altered was cyclin D1, whose expression was highly dependent on AIB1 expression under anchorage-dependent and -independent conditions. Cyclin D1 is an important cell cycle-regulating protein that in response to mitogenic stimulus associates with CDK4/6. The cyclin D1-CDK4/6 complex hyperphosphorylates the retinoblastoma protein, leading to the release of E2F. Free from its association with the retinoblastoma protein, E2F activates genes necessary for cell proliferation (35). Cyclin D1 is a critical downstream target of PI3k-signaling pathway for proliferation in MCF-7 cells (36). It is likely that the reduction in cyclin D1 under low AIB1 conditions would explain some of the cell cycle effects of AIB1 siRNA treatment of MCF-7 cells under anchorage-dependent conditions. However, it appears that the cells are less dependent on cyclin D1 for cell cycle control under anchorage-independent conditions. Our data confirm and extend previous observations that cyclin D1 gene regulation by estrogen is AIB1 dependent (37). In addition, we show that a portion of the basal expression of cyclin D1, as well as its IGF-I induction, occurs independent of estrogen signaling but is nevertheless AIB1 dependent (Fig. 6*B*).

The antiapoptotic protein Bcl-2 was also found in our cDNA array study to be significantly down-regulated in the absence of AIB1. Bcl-2 is a proto-oncogene that is a part of a family of related proteins that functions to either promote or inhibit apoptosis and anoikis (38, 39). In the presence of AIB1 siRNA, Bcl-2 levels were decreased in both basal and IGF-I treatment conditions, regardless of attached or poly-HEMA growth conditions. Bcl-2 is thought to play a central role in the interplay of integrin and IGF-I signaling in anoikis (40, 41), and reductions in Bcl-2 may explain some of the abrogation of the anti-anoikis effect of IGF-I in suspension. Interestingly, Bcl-2 and cyclin D1 expression are interconnected. When Bcl-2 was overexpressed in a human breast epithelial cell line, MCF10A, it caused an increase in the expression of cyclin D1. Bcl-2 was also found to be able to increase the activity of cyclin D1 promoter in both MCF10A and MCF-7 cells independent of anchorage conditions (42). The effects of both the loss of Bcl-2 and AIB1 could therefore contribute to greater reduction in cyclin D1 levels.

Our data indicate that a large portion of the transcriptional control of genes, such as cyclin D1 and Bcl-2, occurs independent of the ER. AIB1 is known to coactivate a number of factors that are not nuclear receptors such as NF-κB (43, 44) and activator protein-1 (21). It is likely that some of these sites are in involved in AIB1 control of basal and IGF-I control of gene transcription in MCF-7 cells. Of note is that both cyclin D1 and Bcl-2 genes are estrogen-inducible genes that contain nonclassical ERE promoters because they do not contain half or full consensus ERE sites in their promoters. Both genes contain in common cAMP-response element, activator protein-1, and Sp-1 sites, which are necessary for estrogen induction of the promoter (29, 33, 45). Furthermore, IGF-I induction of the Bcl-2 promoter is dependent on a cAMP-response element site (46). Thus, it is possible that AIB1 may act at the cAMP-response element, activator protein-1, or Sp-1

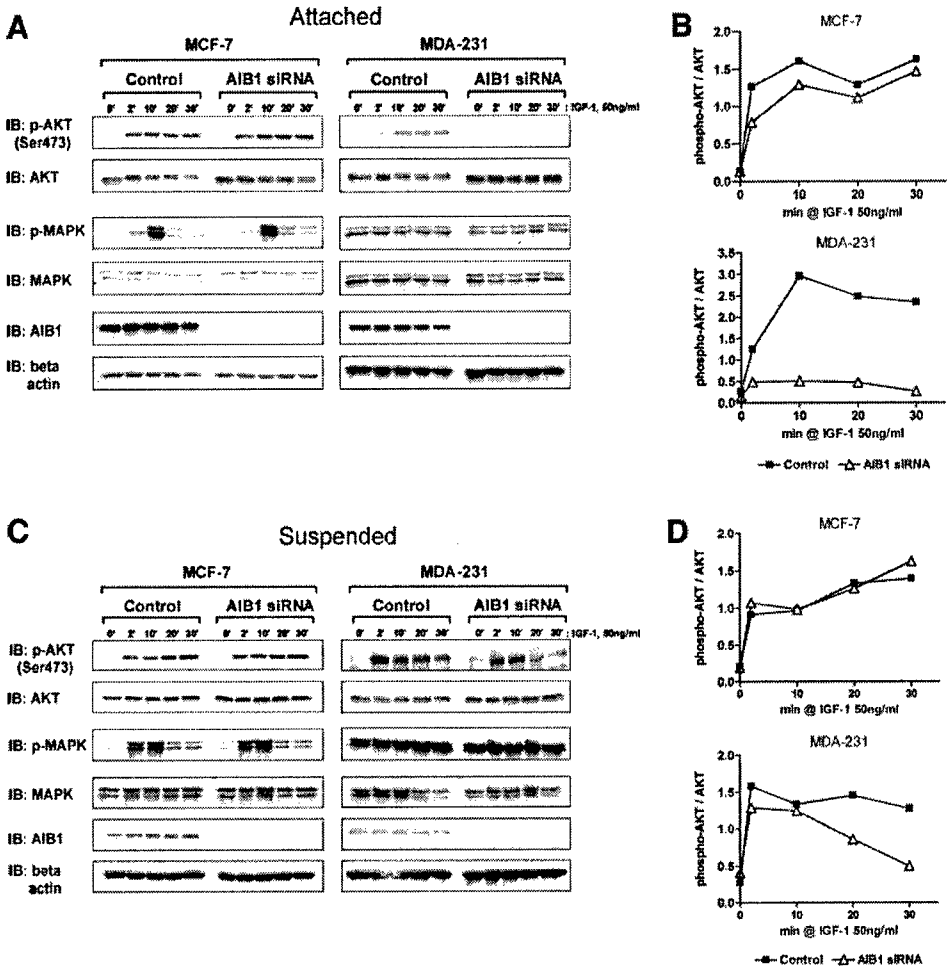

Fig. 8. Role of AIB1 for IGF-I induced AKT and MAPK phosphorylation. *A*. In attached conditions, estrogen-stripped MCF-7 and MDA MB-231 cells were transfected with control or AIB1 siRNA for 48 hours and treated with 50 ng/mL IGF-I. Whole cell lysates were harvested at the indicated time points. *C*. In suspension growth conditions, estrogen-stripped cells were transfected for 18 to 24 hours with siRNA and replated in poly-HEMA (10 μg/mL)–coated dishes for another 24 hours before IGF-I treatment. Whole cell lysates were harvested at the indicated time points. Relative band intensities were assessed using densitometry. Densitometry values were used to calculate the ratio between phosphorylated AKT and total levels of AKT and are represented as line graphs in *B* and *D*.

sites to coactivate expression in the presence of IGF-I, which may not necessitate the presence of the ER.

Although the changes in cyclin D1, Bcl-2, and MAPK could explain the effects of AIB1 siRNA on basal proliferation, it is not clear that these changes would specifically affect the IGF-I *versus* serum pathway. In the analysis of the mouse embryonic fibroblast p/CIP$^{-/-}$ cells, no real changes were observed in IGF-I–signaling molecule pathway molecules (18). Our study of MCF-7 cells indicates that AIB1 plays a role in controlling levels of IGF-IR, and this is especially pronounced under anchorage-independent conditions. In MDA MB-231 cells, however, the IGF-IR levels were unaltered by changes in AIB1 levels and thus do not appear to be involved in AIB1 control of IGF-I proliferation in these cells. As stated above, IGF-IR interplay with the integrin-signaling pathways plays a major role in the control of anoikis in many cell types (47–49), and it appears that AIB1 may be able to potentiate IGF-I inhibition of anoikis in MCF-7 cells by maintaining high IGF-IR levels. Importantly, the maintenance of the high IGF-IR levels occurred even when ER signaling was reduced, suggesting that AIB1 could maintain this phenotype even when breast cancer cells are growing hormone independently. Changes in IRS-1 levels have been observed to be AIB1 dependent in H-*ras*–induced tumors (50), but the decreases in IRS-1 we observed with AIB1 siRNA were small in MCF-7 cells and not observed in the MDA MB-231 cells.

A recent article by Zhou *et al.* (51) found that overexpressing AIB1 caused an increase in AKT levels and an increase in cell size in prostate cancer cells in a steroid-independent manner. In MCF-7 or MDA MB-231 cells, we did observe some changes in unphosphorylated AKT levels but did not observe changes in cell size when AIB1 was down-regulated. Differences in basal AKT regulation between cell types might be explained by differences in PTEN gene status in the cell lines used in these studies. The prostate cancer cell lines, LNCaP and PC-3, used in the Zhou *et al.* (51) study have a defective PTEN gene (52), whereas MCF-7 and MDA MB-231 breast cancer cells have a wild-type PTEN gene (53). It does seem clear from our data that the ability of IGF-I to activate AKT is dependent on AIB1 levels in these breast cancer cell lines at least under certain plating conditions. However, the most profound AIB1-dependent phenotypic change induced by IGF-I is observed when MCF-7 cells are growing anchorage independently. Recall that under these conditions we see little change in the IGF-I activation of AKT, thus it seems likely that AIB1 is also involved in other signaling pathways that predominate when the cells are growing in suspension.

In conclusion, our results suggest that IGF-I induced survival of cells in suspension depends on AIB1 signaling whereas the serum does not. Also, some IGF-I–induced changes in gene expression are dependent on AIB1. The observation that AIB1 is rate-limiting for aspects of IGF-I signaling is important because it implies that AIB1 could effect malignant phenotypic changes induced by growth factors, even if estrogen signaling is not intact. This may become relevant in advanced breast cancer, which is frequently estrogen receptor negative, but has amplified growth factor signaling from the IGF-I–signaling pathways (54). In addition, overexpression of AIB1 may play a role in potentiating growth factor signaling when estrogen signaling is blocked with antiestrogens, thus contributing to the antiestrogen-resistant phenotype in breast cancer. Our studies suggest a broader role of AIB1 in coactivating growth signaling that is not limited to hormonally responsive breast tissue but may be extended to

other tissues that are responsive to IGF-I such as the pancreas (55) and prostate (56).

REFERENCES

1. Onate SA, Tsai SY, Tsai MJ, O'Malley BW. Sequence and characterization of a coactivator for the steroid hormone receptor superfamily. Science (Wash. DC) 1995; 270:1354–7.
2. Voegel JJ, Heine MJS, Zechel C, Chambon P, Gronmeyer H. TIF2, a 160 kDa transcriptional mediator for the ligand dependent activation function AF-2 of nuclear receptors. EMBO J 1996;15:3667–75.
3. Anzick SL, Kononen J, Walker RL, et al. AIB1, a steroid receptor coactivator amplified in breast and ovarian cancer. Science (Wash. DC) 1997;277:965–8.
4. Chen H, Lin RJ, Schiltz RL, et al. Nuclear receptor coactivator ACTR is a novel histone acetyltransferase and forms a multimeric activation complex with P/CAF and CBP/p300. Cell 1997;90:569–80.
5. Li H, Gomes PJ, Chen JD. RAC3, a steroid/nuclear receptor-associated coactivator that is related to SRC-1 and TIF2. Proc Natl Acad Sci USA 1997;94:8479–84.
6. Takeshita A, Cardona GR, Koibuchi N, Suen C-S, Chin WW. TRAM-1, a novel 160-kDa thyroid hormonr receptor activator molecule, exhibits distinct properties from steroid receptor coactivator-1. J Biol Chem 1997;272:27629–34.
7. Suen C-S, Berrodin TJ, Mastroeni R, Cheskis BJ, Lyttle CR, Frail DE. A transcriptional co-activator, steroid co-activator-3 selectively augments steroid receptor transcriptional activity. J Biol Chem 1998;273:27645–53.
8. Henke RT, Haddad BR, Kim SE, et al. Overexpression of the nuclear receptor coactivator AIB1 (SRC-3) during progression of pancreatic adenocarcinoma. Clin Cancer Res 2004;10:6134–42.
9. Sakakura C, Hagiwara A, Yasuoka R, et al. Amplification and over-expression of the AIB1 nuclear receptor co-activator gene in primary gastric cancers. Int J Cancer 2000;89:217–23.
10. Bautista S, Valles H, Walker SL, et al. In breast cancer, amplification of the steroid receptor coactivator gene AIB1 is correlated with estrogen and progesterone receptor positivity. Clin Cancer Res 1998;4:2925–9.
11. Murphy LC, Simon SL, Parkes A, et al. Altered expression of estrogen receptor coregulators during human breast tumorigenesis. Cancer Res 2000;60:6266–71.
12. List HJ, Reiter R, Singh B, Wellstein A, Riegel AT. Expression of the nuclear coactivator AIB1 in normal and malignant breast tissue. Breast Cancer Res Treat 2001;68:21–8.
13. Tikkanen MK, Carter DJ, Harris AM, et al. Endogenously expressed estrogen receptor and coactivator AIB1 interact in MCF-7 human breast cancer cells. Proc Natl Acad Sci USA 2000;97:12536–40.
14. List HJ, Lauritsen KJ, Reiter R, Powers C, Wellstein A, Riegel AT. Ribozyme targeting demonstrates that the nuclear receptor coactivator AIB1 is a rate-limiting factor for estrogen-dependent growth of human MCF-7 breast cancer cells. J Biol Chem 2001;276:23763–8.
15. Lauritsen KJ, List HJ, Reiter R, Wellstein A, Riegel AT. A role for TGF-beta in estrogen and retinoid mediated regulation of the nuclear receptor coactivator AIB1 in MCF-7 breast cancer cells. Oncogene 2002;21:7147–55.
16. Reiter R, Oh AS, Wellstein A, Riegel AT. Impact of the nuclear receptor coactivator AIB1 isoform AIB1-Delta3 on estrogenic ligands with different intrinsic activity. Oncogene 2004;23:403–9.
17. Xu J, Liao L, Ning G, Yoshida-Komiya H, Deng C, O'Malley BW. The steroid receptor coactivator SRC-3 (p/CIP/RAC3/AIB1/ACTR/TRAM-1) is required for normal growth, puberty, female reproductive function, and mammary gland development. Proc Natl Acad Sci USA 2000;97:6379–84.
18. Wang Z, Rose DW, Hermanson O, et al. Regulation of somatic growth by the p160 coactivator p/CIP. Proc Natl Acad Sci USA 2000;97:13549–54.
19. Reiter R, Wellstein A, Riegel AT. An isoform of the coactivator AIB1 that increases hormone and growth factor sensitivity is overexpressed in breast cancer. J Biol Chem 2001;276:39736–41.
20. Bouras T, Southey MC, Venter DJ. Overexpression of the steroid receptor coactivator AIB1 in breast cancer correlates with the absence of estrogen and progesterone receptors and positivity for p53 and HER2/neu. Cancer Res 2001;61:903–7.
21. Torchia J, Rose DW, Inostroza J, et al. The transcriptional co-activator p/CIP binds CBP and mediates nuclear-receptor function. Nature (Lond.) 1997;387:677–84.
22. Bai J, Uehara Y, Montell DJ. Regulation of invasive cell behavior by Taiman, a Drosophila protein related to AIB1, a steroid receptor coactivator amplified in breast cancer. Cell 2001;103:1047–58.
23. McDonald JA, Pinheiro EM, Montell DJ. PVF1, a PDGF/VEGF homolog, is sufficient to guide border cells and interacts genetically with Taiman. Development (Camb.) 2003;130:3469–78.
24. Li G, Fridman R, Kim HR. Tissue inhibitor of metalloproteinase-1 inhibits apoptosis of human breast epithelial cells. Cancer Res 1999;59:6267–75.
25. Bartucci M, Morelli C, Mauro L, Ando S, Surmacz E. Differential insulin-like growth factor I receptor signaling and function in estrogen receptor (ER)-positive MCF-7 and ER-negative MDA-MB-231 breast cancer cells. Cancer Res 2001;61:6747–54.
26. Klotz DM, Hewitt SC, Ciana P, et al. Requirement of estrogen receptor-alpha in insulin-like growth factor-1 (IGF-1)-induced uterine responses and in vivo evidence for IGF-1/estrogen receptor cross-talk. J Biol Chem 2002;277:8531–7.
27. Stoica A, Saceda M, Fakhro A, Joyner M, Martin MB. Role of insulin-like growth factor-I in regulating estrogen receptor-alpha gene expression. J Cell Biochem 2000; 76:605–14.
28. Stewart AJ, Johnson MD, May FE, Westley BR. Role of insulin-like growth factors and the type I insulin-like growth factor receptor in the estrogen-stimulated proliferation of human breast cancer cells. J Biol Chem 1990;265:21172–8.
29. Dong L, Wang W, Wang F, et al. Mechanisms of transcriptional activation of bcl-2 gene expression by 17beta-estradiol in breast cancer cells. J Biol Chem 1999;274: 32099–107.
30. Migliaccio A, Di Domenico M, Castoria G, et al. Tyrosine kinase/p21ras/MAP-kinase pathway activation by estradiol-receptor complex in MCF-7 cells. EMBO J 1996;15: 1292–300.
31. Molloy CA, May FE, Westley BR. Insulin receptor substrate-1 expression is regulated by estrogen in the MCF-7 human breast cancer cell line. J Biol Chem 2000;275: 12565–71.
32. Prall OW, Sarcevic B, Musgrove EA, Watts CK, Sutherland RL. Estrogen-induced activation of Cdk4 and Cdk2 during G_1-S phase progression is accompanied by increased cyclin D1 expression and decreased cyclin-dependent kinase inhibitor association with cyclin E-Cdk2. J Biol Chem 1997;272:10882–94.
33. Sabbah M, Courilleau D, Mester J, Redeuilh G. Estrogen induction of the cyclin D1 promoter: involvement of a cAMP response-like element. Proc Natl Acad Sci USA 1999;96:11217–22.
34. Dauvois S, Danielian PS, White R, Parker MG. Antiestrogen ICI 164,384 reduces cellular estrogen receptor content by increasing its turnover. Proc Natl Acad Sci USA 1992;89:4037–41.
35. Hunter T, Pines J. Cyclins and cancer. II. Cyclin D and CDK inhibitors come of age. Cell 1994;79:573–82.
36. Dufourny B, Alblas J, van Teeffelen HA, et al. Mitogenic signaling of insulin-like growth factor I in MCF-7 human breast cancer cells requires phosphatidylinositol 3-kinase and is independent of mitogen-activated protein kinase. J Biol Chem 1997; 272:31163–71.
37. Planas-Silva MD, Shang Y, Donaher JL, Brown M, Weinberg RA. AIB1 enhances estrogen-dependent induction of cyclin D1 expression. Cancer Res 2001;61:3858–62.
38. Reed JC. Bcl-2 and the regulation of programmed cell death. J Cell Biol 1994;124:1–6.
39. Kluck RM, Bossy-Wetzel E, Green DR, Newmeyer DD. The release of cytochrome c from mitochondria: a primary site for Bcl-2 regulation of apoptosis. Science (Wash. DC) 1997;275:1132–6.
40. Matter ML, Ruoslahti E. A signaling pathway from the alpha5beta1 and alpha(v)beta3 integrins that elevates bcl-2 transcription. J Biol Chem 2001;276:27757–63.
41. Stupack DG, Cheresh DA. Get a ligand, get a life: integrins, signaling and cell survival. J Cell Sci 2002;115:3729–38.
42. Lin HM, Lee YJ, Li G, Pestell RG, Kim HR. Bcl-2 induces cyclin D1 promoter activity in human breast epithelial cells independent of cell anchorage. Cell Death Differ 2001;8:44–50.
43. Werbajh S, Nojek I, Lanz R, Costas MA. RAC-3 is a NF-kappaB coactivator. FEBS Lett 2000;485:195–9.
44. Sheppard KA, Rose DW, Haque ZK, et al. Transcriptional activation by NF-kappaB requires multiple coactivators. Mol Cell Biol 1999;19:6367–78.
45. Liu MM, Albanese C, Anderson CM, et al. Opposing action of estrogen receptors alpha and beta on cyclin D1 gene expression. J Biol Chem 2002;277:24353–60.
46. Pugazhenthi S, Miller E, Sable C, et al. Insulin-like growth factor-I induces bcl-2 promoter through the transcription factor cAMP-response element-binding protein. J Biol Chem 1999;274:27529–35.
47. Doerr ME, Jones JI. The roles of integrins and extracellular matrix proteins in the insulin-like growth factor I-stimulated chemotaxis of human breast cancer cells. J Biol Chem 1996;271:2443–7.
48. Valentinis B, Reiss K, Baserga R. Insulin-like growth factor-I–mediated survival from anoikis: role of cell aggregation and focal adhesion kinase. J Cell Physiol 1998;176:648–57.
49. Frisch SM, Screaton RA. Anoikis mechanisms. Curr Opin Cell Biol 2001;13:555–62.
50. Kuang SQ, Liao L, Zhang H, Lee AV, O'Malley BW, Xu J. AIB1/SRC-3 deficiency affects insulin-like growth factor I signaling pathway and suppresses v-Ha-ras–induced breast cancer initiation and progression in mice. Cancer Res 2004;64:1875–85.
51. Zhou G, Hashimoto Y, Kwak I, Tsai SY, Tsai MJ. Role of the steroid receptor coactivator SRC-3 in cell growth. Mol Cell Biol 2003;23:7742–55.
52. Li J, Yen C, Liaw D, et al. PTEN, a putative protein tyrosine phosphatase gene mutated in human brain, breast, and prostate cancer. Science (Wash. DC) 1997;275:1943–7.
53. Weng LP, Smith WM, Dahia PL, et al. PTEN suppresses breast cancer cell growth by phosphatase activity-dependent G_1 arrest followed by cell death. Cancer Res 1999; 59:5808–14.
54. Dickson RB, Lippman ME. Growth factors in breast cancer. Endocr Rev 1995;16: 559–89.
55. Nair PN, De Armond DT, Adamo ML, Strodel WE, Freeman JW. Aberrant expression and activation of insulin-like growth factor-1 receptor (IGF-1R) are mediated by an induction of IGF-1R promoter activity and stabilization of IGF-1R mRNA and contributes to growth factor independence and increased survival of the pancreatic cancer cell line MIA PaCa-2. Oncogene 2001;20:8203–14.
56. Hellawell GO, Turner GD, Davies DR, Poulsom R, Brewster SF, Macaulay VM. Expression of the type 1 insulin-like growth factor receptor is up-regulated in primary prostate cancer and commonly persists in metastatic disease. Cancer Res 2002;62: 2942–50.